Cubic Mn_2Ga Thin Films: Crossing the Spin Gap with Ruthenium

H. Kurt,[1,*] K. Rode,[1] P. Stamenov,[1] M. Venkatesan,[1] Y.-C. Lau,[1] E. Fonda,[2] and J. M. D. Coey[1]
[1]School of Physics and CRANN, Trinity College, Dublin 2, Ireland
[2]Synchrotron SOLEIL, L'Orme des Merisiers, Saint-Aubin, BP48, 91192 Gif-sur-Yvette Cedex, France
(Received 5 July 2013; published 15 January 2014)

Cubic Mn_2Ga films with the half-Heusler $C1_b$ structure are grown on V (001) epitaxial films. The phase is a soft ferrimagnet, with Curie temperature $T_C = 225$ K and magnetization $M_s = 280$ kA m^{-1}, equivalent to 1.65 μ_B per formula. Adding ruthenium leads to an increase of T_C up to 550 K in cubic Mn_2Ru_xGa films with $x = 0.33$ and a collapse of the net magnetization. The anomalous Hall effect changes sign at $x = 0.5$, where the sign of the magnetization changes and the magnetic easy direction flips from in plane to perpendicular to the film. The $Mn_2Ru_{0.5}Ga$ compound with a valence electron count of 21 is identified as a zero-moment ferrimagnet with high spin polarization, which shows evidence of half-metallicity.

DOI: 10.1103/PhysRevLett.112.027201 PACS numbers: 75.30.Gw, 75.60.Ej, 75.70.-i

Cubic ferrimagnetic Heusler compounds are a rich family of magnetic materials [1], that can exhibit a higher spin polarization at the Fermi level than any binary 3d ferromagnetic alloy. Several Co_2YZ compounds, for example, are thought to be half-metals with a gap in the spin-polarized density of states for one spin direction [1–3], which makes them particularly suitable for spin valves [4,5] and magnetic tunnel junctions [6,7]. The net spin in Bohr magnetons per unit cell should be an integer for a stoichiometric half-metal, and the moments m of X_2YZ half-metals with the $L2_1$ structure are found to follow a modified Slater-Pauling curve [8].

$$m = N_v - 24, \tag{1}$$

where N_v is the number of valence electrons per formula. The ordered $L2_1$ structure illustrated in Fig. 1(a) has four formula units per cubic unit cell, with X in 8c sites, Y in 4b sites, and Z in 4a sites (Cu_2MnAl-type structure). Values of N_v are 3 for Al, Ga, 4 for Si, Ge, Ti, 5 for Sb, As, V, 6 for Cr, 7 for Mn, 8 for Fe, Ru, 9 for Co, and 10 for Ni. Examples are Co_2FeSi ($m = 6\,\mu_B$) [9, 10] and Co_2MnAl ($m = 4\,\mu_B$) [11]. Half Heuslers are compounds with a similar cubic unit cell, but composition XYZ. Half of the 8c sites are usually filled by X atoms in the noncentrosymmetric $C1_b$, MgAgAs-type structure [Fig. 1(b)], but a variant has X and Y atoms ordered on 8c sites (4c/4d), with 4b sites vacant. The modified Slater-Pauling rule is then

$$m = N_v - 18. \tag{2}$$

The original example of a half-metal was NiMnSb ($m = 4\,\mu_B$) [12, 13].

When X and Y atoms carry a moment and the $X-Y$ coupling is antiferromagnetic, the compounds are ferrimagnets. Half-metallic full Heuslers with $N_v = 24$ and half Heuslers with $N_v = 18$ are particularly interesting, because the ferrimagnetism should then be perfectly compensated, with net spin $m = 0\,\mu_B$. At first, such a metal with perfect spin polarization was termed a "half-metallic antiferromagnet," although the two sublattices are strictly inequivalent, structurally and often chemically. If it existed, it could be useful because the material would be fully spin polarized, yet would be free from shape anisotropy and create no stray field [14].

Although there have been numerous electronic structure calculations for hypothetical compounds with perfectly compensated ferrimagnetism [1, 14–19], all attempts to make them in practice have failed [14]. Nature seems to shun this unusual variety of magnetic order. Half-metallicity is a zero-temperature property, which can be spoiled by imperfect atomic order of the X, Y, and Z atoms in the structure, spin-orbit coupling, or finite temperature, either due to smearing of the Fermi surface or to the different temperature dependence of the magnetization of the two sublattice magnetizations [16]. Candidate materials with the requisite number of valence electrons either turn out to have almost no moment on the transition metal (e.g., Fe_2VGa [20]), or else they decompose (e.g., Co_2CrGa [21]), or do not crystallize in a cubic Heusler structure and consequently exhibit a net magnetization (e.g., Mn_3Ga, Cr_2FeGe, Mn_2Ge, Mn_2Sn, and CrMnSb). Strategies to avoid these difficulties have been to deposit thin films on a substrate or seed layer with a suitable lattice parameter [22] or to use high-energy ball milling to make a bulk disordered cubic precursor [20]. The first approach is useful for spintronics, and we adopt it here to make a new type of Heusler compound with formula X_2Y_xZ, focusing on the $x = 0.5$ composition with 21 valence electrons.

A cubic phase of ordered Mn_2Ga or Mn_3Ga has not been observed in the bulk. Here, we are able to make cubic Mn_2Ga films with the $C1_b$ structure. Ruthenium addition leads to magnetically ordered films at room temperature, with tunable magnetization and magnetic anisotropy. The

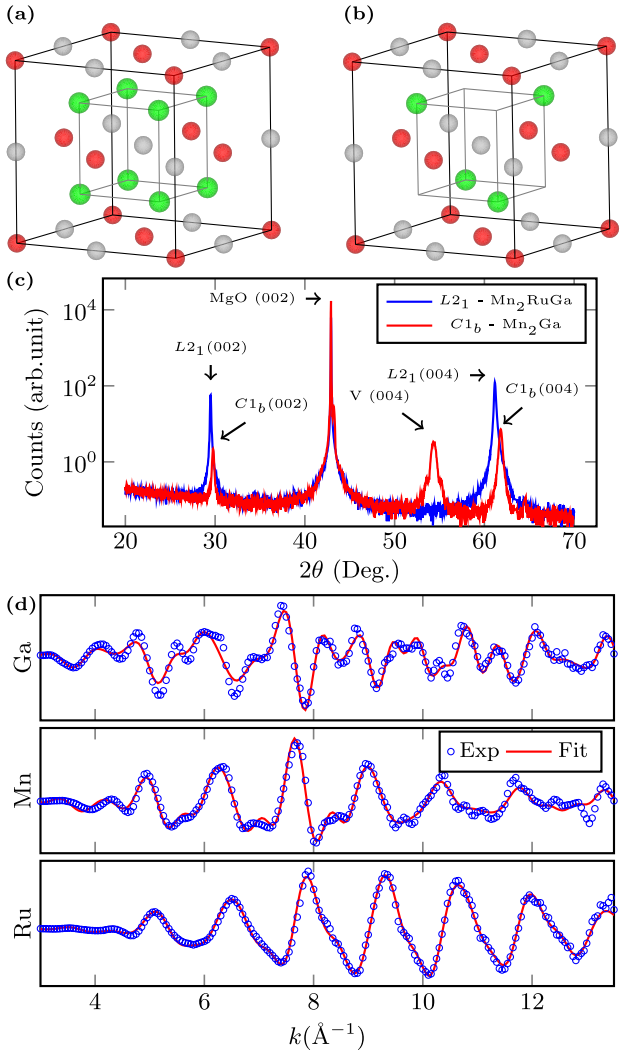

Fig. 1 (color online). (a) Crystal structure of an $L2_1$ full Heusler X_2YZ with X (green), Y (gray), and Z (red) occupying $8c$, $4b$, and $4a$ positions. (b) A $C1_b$ half-Heusler XYZ with X, Y, and Z occupying $4c$, $4b$, and $4a$ positions. (c) X-ray diffraction patterns of $C1_b$-Mn_2Ga and $L2_1$-Mn_2RuGa thin films grown on MgO (001) substrates. The $C1_b$ phase is grown on a (001) oriented vanadium seed layer. (d) Extended x-ray absorption fine structure at the K edges of a $Mn_2Ru_{0.52}Ga$ sample. Fits are discussed in the text.

films were grown on MgO (001) substrates by dc-magnetron sputtering at 350 °C in a Shamrock high-vacuum deposition system with a base pressure of 2×10^{-8} Torr. They were cosputtered from a Ru target and a stoichiometric Mn_2Ga target at a rate of ~1 nm/min, by varying the sputtering power of Ru while keeping the Mn_2Ga sputtering power constant, and then covered by a 2–3 nm thick MgO layer to prevent oxidation. Films of cubic Mn_3Ga were sputtered from a stoichiometric Mn_3Ga target. Both Mn_2Ga and Mn_3Ga were grown on a V (001) seed layer while all other films grew directly on MgO. The composition was determined by energy dispersive x-ray analysis and mass spectroscopy.

The Mn_2Ru_xGa films were 60–185 nm thick, with a rms roughness of 0.3–0.5 nm. X-ray diffraction data are shown in Fig. 1(c). The lattice parameter perpendicular to the sample surface $a_\perp$ is found to vary from 598 to 606 pm depending on Ru concentration. Reciprocal space maps and ϕ scans were used to determine the in-plane lattice constant $a_{||}$, and the epitaxial relation with the MgO substrate. A clear reflection from the thin film is found at the azimuthal angle ϕ corresponding to the MgO [110] in-plane direction. This could be identified as either a [hhl], or a [h0l] reflection from the thin film. Assuming it is [h0l], we find that the in-plane lattice parameter is 596 pm, so the film is essentially cubic with substrate-induced strain of order 1%.

The extended x-ray absorption fine structure (EXAFS) signal was measured on the Ga, Mn, and Ru K edges, and the results are shown in Fig. 1(d). To fit the data, we began with a model where Mn occupies two inequivalent sites, $4b$ and $4c$, in a 2×2 $C1_b$ supercell, while Ga occupies $4a$ sites and Ru occupies half of the remaining, $4d$ sites. The atoms were then allowed to change places at random, using a reverse Monte Carlo method, and the EXAFS was simulated including multiple scattering up to 0.7 nm. The simultaneous least-squares fits of the three data sets in Fig. 1(d) are excellent; the fitted structure is pseudocubic with lattice parameters of 597, 597, and 603 pm. The Ru and Ga remain in separate planes and there are no Ru-Ru or Ga-Ga nearest-neighbor contacts, which is consistent with a $C1_b$ or $L2_1$ structure.

Magnetization was measured using a 5 T superconducting quantum interference device or a 14 T vibrating sample magnetometer. Data were corrected for the MgO substrate contribution, which shows a paramagnetic Curie-law upturn at low temperature due to Fe^{2+} impurities. No demagnetizing correction was applied in the out-of-plane measurement. The Curie temperature of cubic $C1_b$-Mn_2Ga is 225 ± 10 K as shown in Fig. 2(a). Ruthenium addition raises the Curie temperature above room temperature as shown in the T_C vs x curve in Fig. 2(c). The magnetization and magnetic anisotropy also vary remarkably as a function of Ru concentration, as illustrated by the magnetization curves in Fig. 2(b). The magnetization falls practically to zero (21 kA m^{-1} or ≈ 0.1 μ_B/formula) at $x = 0.48$ and then rises again with increasing x, which we interpret in Fig. 2(c) as a change of sign of the magnetization. This demonstrates that the perfectly compensated ferrimagnetic state lies close to $x = 0.5$, where the valence electron count is 21. The anisotropy appears to correlate with $a_\perp$, and it changes from in-plane to perpendicular between $x = 0.48$ and $x = 0.52$ at a lattice parameter of 601 pm. The reversal of magnetic anisotropy is illustrated by magnetization measurements of samples with two different ruthenium concentrations in Fig. 2(b). Appreciable coercivity appears in the easy-axis hysteresis loops of the samples with the lowest magnetization.

Mn_3Ga films were also cubic, with a lattice parameter of 591 pm. They have a granular structure, with in-plane

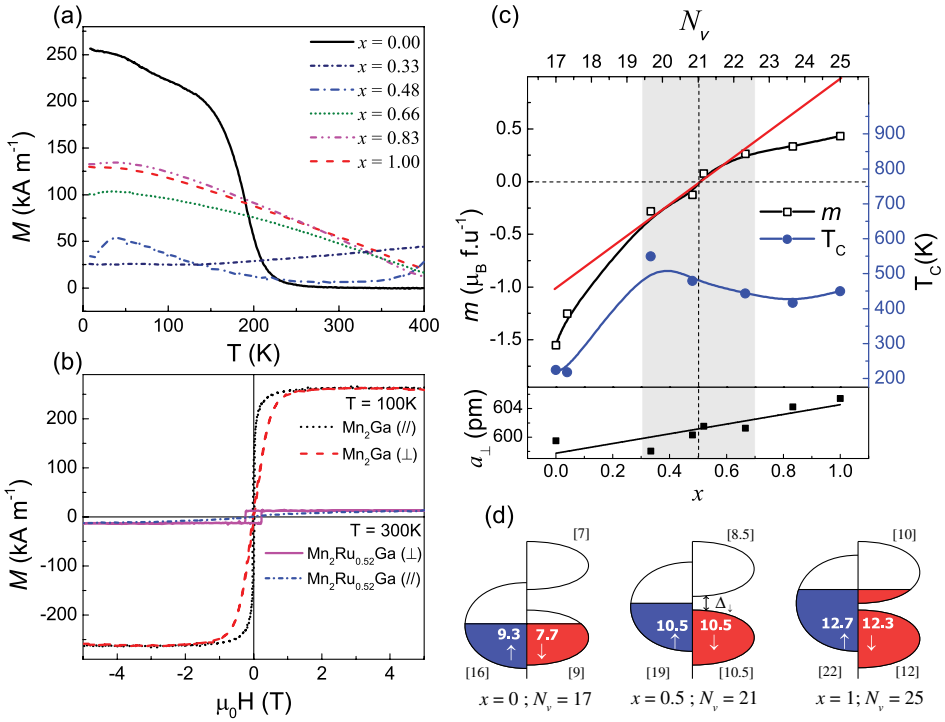

Fig. 2 (color online). (a) Thermal scans in 200 mT of the magnetization of $C1_b$-Mn_2Ru_xGa films with different Ru content. (b) In-plane and perpendicular magnetization of a cubic $C1_b$-Mn_2Ga film at 100 K and a $Mn_2Ru_{0.52}Ga$ film at 300 K. (c) Variation of Curie temperature and moment with Ru concentration x and number of valence electrons per formula unit. The magnetic anisotropy changes from in-plane to perpendicular when $x > 0.5$, and the moment is reversed in sign. Its variation close to $x = 0.5$ is indicated by a red line with slope 2. The half-metallic region is lightly shaded. The lower panel shows the variation of the lattice parameter $a_\perp$, normal to the substrate, as a function of x. (d) Schematic density of states showing the effect of Ru addition in Mn_2Ru_xGa, which illustrates the Fermi level crossing the spin gap.

anisotropy, and a ferrimagnetic magnetization of 90 kA m^{-1} (0.53 μ_B/formula) at 300 K.

Figure 2(d) summarizes the effect of ruthenium addition in Mn_2Ru_xGa on the density of states. For Mn_2Ga, the spin gap $\Delta_\downarrow$ in the $\downarrow$ band lies a few tenths of an eV above the Fermi level E_F. Ruthenium adds both states and electrons to the compound, so that the Fermi level falls in the spin gap for $x = 0.5$. Further Ru addition then drives E_F all the way across the gap, so that the compounds are half-metals only in the range $0.3 \leq x \leq 0.7$. The number of available states—based on a total of 12 for Mn or Ru and 8 for Ga—is shown in square brackets, and electron occupancy of the $\uparrow$ and $\downarrow$ bands indicated by the white figures is based on the measured magnetic moments. The spin gap is mainly due to hybridization of the one-electron $3d$ states, and all six p states of Ga lie well below the Fermi level [18,19].

The resistivity, magnetoresistance, and Hall effect were measured on 100 μm Hall bars of several compositions. Data for the $x = 0.33$ and $x = 0.83$ samples are shown in Fig. 3. The sign of the anomalous Hall effect is opposite for these two compositions, confirming the change in sign of the magnetization shown in Fig. 2(c). Furthermore, it changes sign at 200 K for $x = 0.48$; the anomalous Hall coefficient is several times greater in the half-metal, $x = 0.33$, than the metal, $x = 0.83$. The strong temperature dependence of the normal Hall coefficients (factors of 8 and 3, respectively) indicates that the Fermi level lies close to the band edge (on the order of 20 meV), whereas the field dependence of the magnetoresistance supports the idea that at least two different Fermi surface pockets participate in the transport. There is some evidence of a downturn in the temperature dependence of the resistivity, for $x = 0.33$ above about 300 K, in agreement with the upturn in magnetization, shown in Fig. 2(a), and subject to the same characteristic energy scale.

We measured the spin polarization of two samples of composition $Mn_2Ru_{0.48}Ga$ and Mn_2RuGa using point contact Andreev reflection (PCAR) spectroscopy [23,24]. The $x = 0.48$ sample with the very small magnetization ($M_s = 21$ kA m^{-1}) and in-plane anisotropy shows 54% spin polarization at the Fermi level, significantly higher than 41% for the $x = 1.0$ sample which has $M_s = 75$ kA m^{-1}, as shown in Fig. 4.

Although 54% spin polarization is well short of the 100% expected for a half-metal, it is close to the maximum that has been measured by PCAR on any Heusler compound. Diffusive spin polarization measurements on bulk and thin-film Heusler alloys are never much in excess of

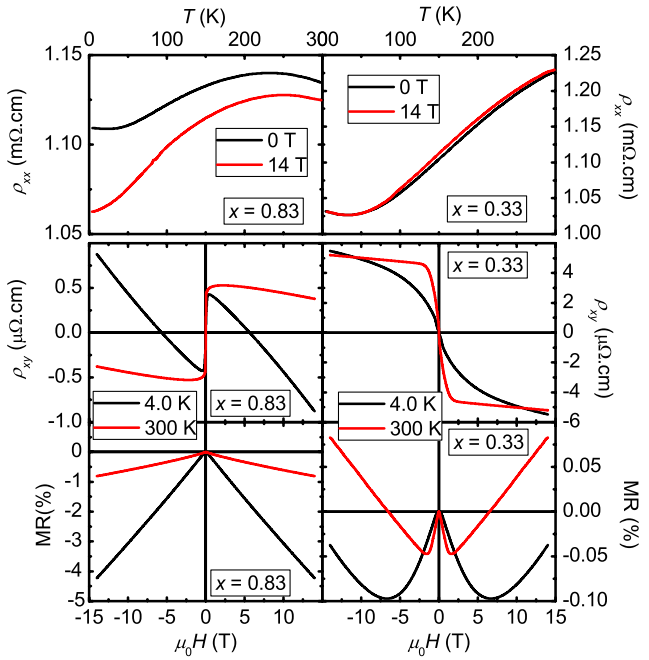

Fig. 3 (color online). Transport on half-metallic $Mn_2Ru_{0.33}Ga$ (right) and metallic $Mn_2Ru_{0.83}Ga$ (left) showing evidence of the change of magnetic and electronic structure on crossing the spin gap. Panels show resistivity (top), Hall effect (middle), and magnetoresistance (bottom).

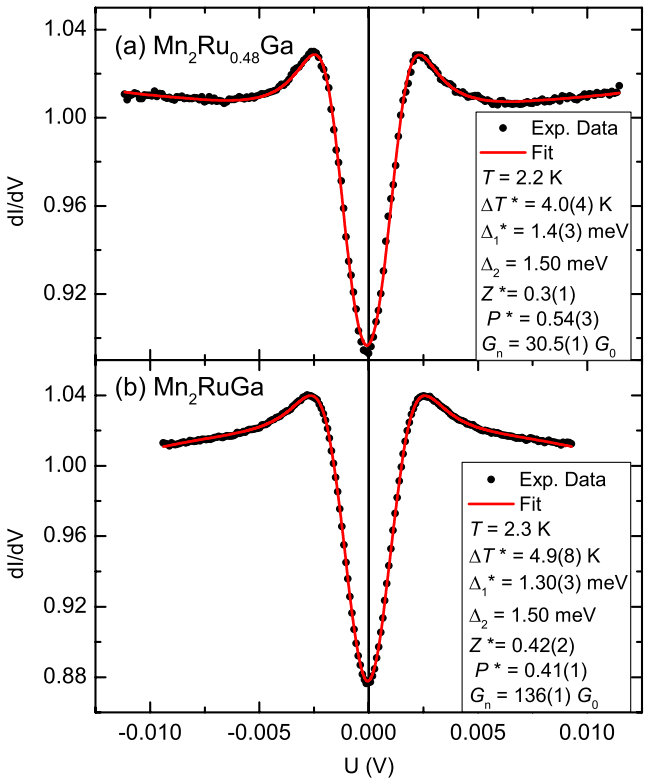

Fig. 4 (color online). (a) Point contact Andreev reflection spectroscopy of cubic $Mn_2Ru_{0.48}Ga$ film with in-plane anisotropy and (b) cubic Mn_2RuGa with perpendicular anisotropy.

60% [10,23,25], probably because the band dispersion is different for the surface and the bulk, or because of spin-orbit scattering. Recent measurements on Co_2FeSi, for example, yielded 51% [10]. The fitting model takes full account of a number of parameters such as series resistance, superconducting proximity effect, and electronic heating, as described previously [24].

The valence-electron rule for the magnetization of half-metallic half-Heusler compounds was given by Eq. (2). The rule predicts a moment of $(-)1\ \mu_B$ for Mn_2Ga, which is less than the measured value of 1.65 μ_B. For full Heuslers, the rule was given by Eq. (1), which predicts a moment of 1 μ_B for $x = 1$ compared with the 0.44 μ_B measured, which is again incompatible with a half-metallic state. However, the slope of the $M(x)$ curve in the zone where the moment changes sign, indicated by the red line in Fig. 2(c), is precisely that expected for a half-metal. The vanishing of the moment of the Mn_2Ru_xGa alloy is evidence that it is a fully compensated ferrimagnet; the fact that this occurs at $x = 0.5$ where the valence electron count is 21, together with the slope of the $m(x)$ curve at $x = 0.5$ is the best evidence that we have actually found a zero-moment band half-metal.

It is very unlikely that the small magnetization of these films could be due to a sudden collapse of the Mn atomic moments at $x = 0.5$, comparable to the vanishing Fe moment in Fe_2VGa [20]. There is an anomalous Hall effect, but no lattice parameter anomaly at $x = 0.5$. The Mn($4c$)-Mn($4b$) distance of 259 pm corresponds to an antiferromagnetic direct exchange integral. Mn on $4b$ sites in Heusler alloys tends to have a moment of about 3 μ_B, whereas for Mn on $4c/4d$ sites it is about 1.5 μ_B. These values have been measured by neutron diffraction on bulk samples of Co_2MnGa [26], Mn_2VAl [27], and tetragonally distorted Mn_3Ga [28], as well as by XMCD on $Mn_{3-\delta}Ga$ thin films [28].

In conclusion, we have stabilized thin films of a new cubic Mn_2Ga phase with the $C1_b$ structure. Ruthenium can be added without significant change of the lattice parameter, and the magnetization, anisotropy and anomalous Hall coefficient all change sign at a Ru content $x = 0.5$, where $N_v = 21$. The Slater-Pauling rule predicts a perfectly compensated ferrimagnet at this concentration, which is consistent with our results constituting the first good experimental evidence for a fully compensated half-metal. With improved mastery of the atomic order and composition, and both chemical pressure and substrate-induced strain in this, or related $X_2Y_{0.5}Z$ compounds such as $Mn_2Fe_{0.5}Al$, it may be possible to combine the controllable anisotropy and low net magnetization with an increased Curie temperature and improved spin polarization. Already, our device quality low-moment Mn_2Ru_xGa films with $x \approx 0.5$ offer some interesting possibilities for device applications such as spin-torque

switched memory elements, and spin torque oscillators where damping is controlled by emission losses.

This work was supported by Science Foundation Ireland as part of the NISE project (10/IN1.13006), and conducted under the framework of the INSPIRE programme and the SSPP project (11/SIRG/I2130), funded by the Irish Government's Programme for Research in Third Level Institutions, Cycle 4, National Development Plan 2007-2013. Support is also provided by Synchrotron SOLEIL through Proposal No. 20110285. K. R. acknowledges financial support from the EU FP7 project IFOX (NMP3-LA-2010-246102).

*Present address: Department of Engineering Physics, Istanbul Medeniyet University, 34720 Istanbul, Turkey.
huseyin.kurt@medeniyet.edu.tr

[1] T. Graf, J. Winterlik, L. Müchler, G. H. Fecher, C. Felser, and S. S. P. Parkin, in *Handbook of Magnetic Materials*, edited by K. H. J. Buschow (Elsevier, Amsterdam, 2013), Vol. 21, p. 1.
[2] J. Kübler, A. R. Williams, and C. B. Sommers, Phys. Rev. B **28**, 1745 (1983).
[3] S. Chadov, G. H. Fecher, C. Felser, J. Minár, J. Braun, and H. Ebert, J. Phys. D **42**, 084002 (2009).
[4] Y. K. Takahashi, A.Srinivasan, B. Varaprasad, A. Rajanikanth, N. Hase, T. M. Nakatani, S. Kasai, T. Furubayashi, and K. Hono, Appl. Phys. Lett. **98**, 152501 (2011).
[5] T. Iwase, Y. Sakuraba, S. Bosu, K. Saito, S. Mitani, and K. Takanashi, Appl. Phys. Express **2**, 063003 (2009).
[6] Y. Sakuraba, M. Hattori, M. Oogane, Y. Ando, H. Kato, A. Sakuma, T. Miyazaki, and H. Kubota, Appl. Phys. Lett. **88**, 192508 (2006).
[7] W. Wang, H. Sukegawa, R. Shan, S. Mitani, and K. Inomata, Appl. Phys. Lett. **95**, 182502 (2009).
[8] J. Kübler, *Theory of Itinerant Electron Magnetism* (Clarendon Press, Oxford, 2000).
[9] M. Oogane, Y. Sakuraba, J. Nakata, H. Kubota, Y. Ando, A. Sakuma, and T. Miyazaki, J. Phys. D **39**, 834 (2006).
[10] L. Makinistian, M. M. Faiz, Raghava P. Panguluri, B. Balke, S. Wurmehl, C. Felser, E. A. Albanesi, A. G. Petukhov, and B. Nadgorny, Phys. Rev. B **87**, 220402 (2013).
[11] J.-C. Tung and G.-Y. Guo, New J. Phys. **15**, 033014 (2013).
[12] R. A. de Groot, F. M. Mueller, P. G. van Engen, and K. H. J. Buschow, Phys. Rev. Lett. **50**, 2024 (1983).
[13] K. Hanssen, P. Mijnarends, L. Rabou, and K. Buschow, Phys. Rev. B **42**, 1533 (1990).
[14] X. Hu, Adv. Mater. **24**, 294 (2012).
[15] I. Galanakis and P. Mavropoulos, J. Phys. Condens. Matter **19**, 315213 (2007).
[16] E. Şaşıoğlu, Phys. Rev. B **79**, 100406 (2009).
[17] M. Shaughnessy, L. Damewood, C. Y. Fong, L. H. Yang, and C. Felser, J. Appl. Phys. **113**, 043709 (2013).
[18] I. Galanakis, P. H. Dederichs, and N. Papanikolaou, Phys. Rev. B **66**, 174429 (2002).
[19] I. Galanakis, P. H. Dederichs, and N. Papanikolaou, Phys. Rev. B **66**, 134428 (2002).
[20] M. Hakimi, M. Venkatesan, K. Rode, K. Ackland, and J. M. D. Coey, J. Appl. Phys. **113**, 17B101 (2013).
[21] M. Meinert and M. P. Geisler, J. Magn. Magn. Mater. **341**, 72 (2013).
[22] S. Kämmerer, A. Thomas, A. Hütten, and G. Reiss, Appl. Phys. Lett. **85**, 79 (2004).
[23] R. J. Soulen Jr. *et al.*, Science **282**, 85 (1998).
[24] P. Stamenov, J. Appl. Phys. **111**, 07C519 (2012).
[25] H. Kurt, K. Rode, M. Venkatesan, P. S. Stamenov, and J. M. D. Coey, Phys. Rev. B **83**, 020405 (2011).
[26] P. J. Webster, J. Phys. Chem. Solids **32**, 1221 (1971).
[27] H. Itoh, H. Itoh, T. Nakamichi, Y. Yamaguchi, and N. Kazama, Trans. Jpn. Inst. Met. **24**, 265 (1983).
[28] K. Rode *et al.*, Phys. Rev. B **87**, 184429 (2013).